Global sensitivity analysis of acoustic transmission models through infinite plates

J.-L Christen [1], **M. Ichchou** [1], **B. Troclet** [2], **M. Ouisse** [3]
[1] École Centrale Lyon, LTDS
36 avenue Guy de Collongue, 69134 Écully, France
e-mail: **jean-loup.christen@ec-lyon.fr**

[2] Airbus Defence and Space
66, Route de Verneuil 78133 Les Mureaux Cedex, France

[3] FEMTO-ST Institute, Department of Applied Mechanics
24 rue de l' Épitaphe, 25000 Besançon, France

Abstract
Noise reduction is a particularly important issue in the aerospace industry, as the very harsh acoustic environment inside the launcher may damage the payload, especially at lift-off. In order to optimize the noise level inside the payload cavity of a launcher, it is important to study the acoustic transmission through the fairing in a broadband frequency range. Acoustic models may depend on many different and independent design parameters, such as materials and geometry. At early design stages, these parameters can vary in broad ranges. In order to reduce the number of parameters of the model, global sensitivity analysis (GSA) is therefore needed to identify the most influential ones. A method for GSA of sound transmission to design parameters is proposed in this paper. One of the most promising class of global sensitivity analysis methods is the Analysis of variance (ANOVA) family, which require a high number of calls to the model function. As this is quite expensive to run, a first step is to build a metamodel of the system. The kriging technique has been retained for this study. This metamodel is then used to perform a global sensitivity analysis with the Fourier Amplitude Sensitivity Test (FAST) method.

1 Introduction

Noise reduction is a very important issue in the industry. Typical applications include interior noise inside plane fuselage or car bodies, or payload comfort for space launchers. Transmission loss through complex structures has been studied extensively throughout the last 40 years. The considered structures range from plates [1] to multilayered composite cylindrical shell [2]. More recently, numerical models based on the Wave finite element method [3] or taking into account periodicity of the structure [4] have been proposed.

As complexity of the structure increases, so does the number of parameters needed to accurately model its behavior. However, given industrial constraints, the design range of all these parameters may be so that some of them have major influence on the model output while the effect of others remains small. If these parameters can be identified and fixed to a reference value, the optimization problem need only be conducted on a reduced design space, thus saving computing time.

Several methods have been proposed for optimizing noise transmission through composite structures. Wang et al. [5] propose an application of genetic algorithm to find an optimal design of sandwich panel considering both structural and acoustic constraints. However, in order to be efficiently designed, these methods need a good insight in the mechanical behavior of the model with respect to its parameters.

Global sensitivity analysis (GSA) methods have been studied since the 70's for different purposes. Cukier et al. [6] developed the FAST method to study complex chemical reactions. Iooss et al. [7] used sensitivity analysis on radiologic risk assessment models. Ouisse et al. [8] applied the FAST method to porous material models, regarding acoustic impedance and absorption.

The main drawback of GSA methods is usually that they are very computationally intensive, as they rely on the evaluation of a generally complex computer model at a large number of design points. One way to overcome this limitation is to build a metamodel prior to the analysis, as proposed for example by Marrel et al. [9, 10]. Metamodeling is the process of replacing a complex physical model by an estimate based on the computation of a reduced number of points. Several techniques exist, such as support vector machines, neural networks and Gaussian process modeling. A benchmark of their performances can be found in [11]. Gaussian process modeling, also known as kriging, has several advantages, such as exact interpolation at the learning points, an ability to provide an estimate of the metamodeling error, and being rather easy to implement. The DACE toolbox implementation [12] has been used for the present study.

Contrarily to other models to which GSA has been applied, the ranking of parameters by order of influence on the output given by sensitivity analysis is not absolute in acoustic models, but depends on frequency. As the frequency ranges considered for noise transmission may be quite wide, the system will present very different behaviors in different regions of the excitation spectrum. The behavior in low frequencies is essentially governed only by the mass of the system, while damping and stiffness-like parameters will play a more important role for higher frequencies. However, the transition between these phases can be rather complex. The objective of this paper is to find interpretations of the results of sensitivity analysis applied to acoustic transmission models for systems of increasing complexity.

The paper is structured as follows. Section 2 presents an overview of the global sensitivity analysis method used in this work. It combines the FAST technique with a metamodeling step. Section 3 presents a 4-parameter model of acoustic transmission loss through an infinite isotropic plate under oblique plane wave excitation, and the results of a FAST analysis of that model. Section 4 presents the same kind of results on a 6-parameter model of orthotropic plate under diffuse field excitation.

Finally conclusions are summarized in section 5.

2 Global sensitivity analysis

2.1 Analysis of variance

In the analysis of variance technique, a parameter's influence on the model output is quantified by the impact it has on the variance in the given design range. In the following development, a generic mathematical model is considered. A model is a real valued function f defined over K^n, where $K = [0, 1]$. With appropriate scaling and translations, any model defined over continuous ranges of parameters can be represented that way.

For a given model f linking input parameters $\mathbf{x} = (x_1, ...x_n)$ to a scalar output $y = f(\mathbf{x})$, there exists a unique partition of f so that

$$y = f(x_1, x_2, ...x_n) = f_0 + \sum_{i=1}^{n} f_i(x_i) + \sum_{i<j} f_{ij}(x_i, x_j) + ... + f_{1...n}(x_1, ..., x_n) \tag{1}$$

provided that each function f_I involved in the decomposition has zero mean over its range of variation

$$\int_{K|_I} f_I(x_I) \mathrm{d}x_I = 0. \tag{2}$$

The decomposition given by equation 1 is called the Hoeffding decomposition or high order model representation (HDMR).

For a given set of indices $I = \{i_1, \ldots, i_n\}$, the partial variance is therefore the variance of f_I

$$D_I = \int_{K|_I} f_I(x_I)^2 \mathrm{d}x_I \tag{3}$$

the sensitivity index relative to the set I is expressed as the ratio of the variance of the function f_I to the total variance of the model:

$$\mathrm{SI}(I) = \frac{D_I}{D}. \tag{4}$$

The computation of all the 2^n sensitivity indices is needed to represent completely the model, however this becomes quickly a very costly task in terms of computational time, as they have to be evaluated by numerical integration. However, most information about a parameter's influence can be found in the first-order sensitivity index and the total sensitivity index, which can be computed more efficiently with the FAST method.

For a given parameter $i \in [1, n]$, the main effect (ME) is then the sensitivity index relative to the 1-dimensional function f_i. Another interesting sensitivity measure for a given parameter i is the total sensitivity index, defined as the sum of the indices of all sets of parameters I to which i belong.

$$\mathrm{TSI}(i) = \sum_{\substack{I \subset [1,n] \\ i \in I}} \mathrm{SI}(I) \tag{5}$$

2.2 Interpretation

The first-order index represents the share of the output variance that is explained by the considered parameter alone. Most important parameters therefore have high ME, but a low ME does not mean the parameter has no influence, as it can be involved in interactions.

The total index is a measure of the share of the variance that is removed from the total variance when the considered parameter is fixed to its reference value. Therefore parameters with low TSI can be considered as non-influential.

2.3 Main effect computation

The idea of the FAST method is to avoid the evaluation of the n-dimensional integrals needed for the computation of the f_i functions, and replace them by a single 1-dimensional integral along a *space-filling* curve in the design space. This curve is defined so as to be periodic with different periods relative to each parameter. Saltelli [13] propose the sampling function defined by:

$$x_i = \frac{1}{2} + \frac{1}{\pi} \arcsin\left(\sin\left(\omega_i s + \varphi_i\right)\right) \tag{6}$$

The frequencies ω_i are integers chosen so as to minimize interference between parameters. The frequencies are said to be free of interference up to order M if all linear combinations

$$\sum_{i=1}^{n} \alpha_i \omega_i \neq 0 \tag{7}$$

where $\alpha_i \in \mathbb{Z}$ and $\sum_{i=1}^{n} |\alpha_i| < M$.

As all frequencies are integers, the resulting function is 2π-periodic with respect to variable s. The sampling is then done using $N > 2\omega_n + 1$ samples in the $[0, 2\pi]$ interval. Calling $y_k = f(x_k)$ the model output on each sample, the discrete Fourier transform $\hat{y}_k$ can be computed.

The total variance of the function in the design space is computed with Parseval's theorem as

$$D = \int_K f^2(x) - f_0^2 \mathrm{d}x \approx \sum_{k=1}^{N} y_k^2 = \sum_{k=1}^{N} \hat{y}_k^2 \tag{8}$$

The contribution of parameter i will then be:

$$D_i = \sum_{k=1}^{M} \hat{y}_{k\omega_i} \tag{9}$$

2.4 Total sensitivity index computation

A method proposed in [13] is to assign one frequency ω_i to parameter i and another $\omega_{\sim i}$ to all other parameters. The same sampling curve as defined in equation 6 is used with these two frequencies only. The total sensitivity index of parameter i is then

$$TSI(i) = 1 - \frac{D_{\sim i}}{D} \tag{10}$$

where $D_{\sim i}$ is the partial variance relative to all parameters but i.

2.5 Gaussian process metamodeling

In order to avoid too long computations, it is possible to run the FAST algorithm on a metamodel rather than on the full computer code. The learning points for the metamodel are chosen using an optimized Latin hypercube sampling [14], so that all parts of the design space are sampled equally. The problem can now be stated as follows: knowing the exact value of the model at m trial points $y_j = f(\mathbf{x}_j)$, we want to estimate the value $y = f(\mathbf{x})$ for any $\mathbf{x} \in K^n$.

The Gaussian process metamodeling [15] is based on a decomposition of the model function into a regression part and a "stochastic part". Polynomial regression is usually considered for the former part, so that we can write:

$$f(\mathbf{x}) = P(\mathbf{x}) + Z(\mathbf{x}). \tag{11}$$

where $P(\mathbf{x}x)$ is a polynomial in with respect to the components of $\mathbf{x}$. In our case, we assume a zero-order polynomial regression, so that $P(x) = \sum_{i=1}^{m} y_i/m$ is a constant scalar, taken to the mean value of the function over its definition set.

The stochastic part $Z(\mathbf{x})$ is assumed to be a centered stationary Gaussian process, meaning that the value at one point depends only on the distance to the other points. It is characterized by its covariance function σ. The word "stationary" means here that the covariance function depends only on the distance between the considered points. The covariance between two points is then

$$\mathrm{cov}(\mathbf{x}_i, \mathbf{x}_j) = \prod_{k=1}^{n} \sigma\left(\theta \left| x_i^{(k)} - x_j^{(k)} \right|\right) \tag{12}$$

where θ is a parameter defining the distance in the parameter space at which two parameters are independent of each other. The DACE toolbox [12] estimates it with a maximum of likelihood estimator.

Once the covariance function is chosen, the estimated value at the new point $\mathbf{x}$ is calculated by $\hat{y} = \sum_{i=1}^{n} \lambda_i y_i$. The optimal weights λ_i are chosen with a maximum of likelihood estimator [15], so that:

$$\lambda = \Gamma^{-1}\left(\gamma + \mathbf{1}\frac{1 - \mathbf{1}'\Gamma^{-1}\gamma}{\mathbf{1}'\Gamma\mathbf{1}}\right), \tag{13}$$

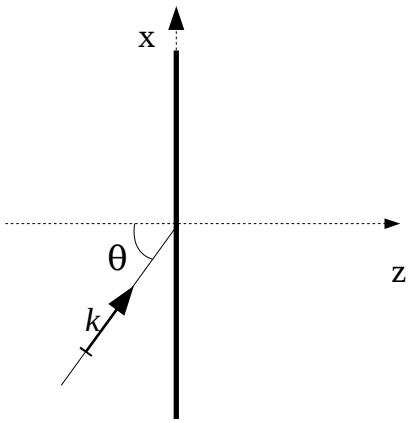

Figure 1: Infinite plate impinged by an oblique plane wave

where Γ is the matrix of covariances between trial points $\Gamma_{ij} = \mathrm{cov}(\mathbf{x}_i, \mathbf{x}_j)$, and γ is the vector of covariances between the points to be estimated and the known points $\gamma_i = \mathrm{cov}(\mathbf{x}_i, \mathbf{x})$.

The spherical covariance function

$$\sigma(r) = \begin{cases} 1 - 1.5r + 0.5r^3 & \text{if } r \leqslant 1 \\ 0 & \text{if } r > 1 \end{cases} \tag{14}$$

is preferred for our case, as it is continuously differentiable, but non-zero only on a compact domain, meaning that the contribution of points far away from the estimate is exactly zero. Thus, the matrix Γ and correlation γ are sparse and the computation is eased when m is high.

In our applications, $m = 1000$ will be used.

2.6 Frequency-band averaging

In most of the cases studied here, there exist regions of the design space where damping is low, and therefore the transmission loss may exhibit locally very sharp variations for some frequencies. Because of the reduced number of samples, a metamodel may not be able to represent correctly these variations. However, the acoustic quantity of interest considered in this work, sound transmission loss (TL) is usually computed in frequency bands, and not at particular frequencies.

This technique allows to overcome the limitation highlighted before: as the response varies much more slowly when averaged over a frequency band, it can be represented more accurately with a computationally cheaper metamodel.

3 Isotropic plate

3.1 Plane wave excitation

3.1.1 Model

The first case to be considered is that of the acoustic transmission through an infinite isotropic plate, shown in figure 1 The unbounded plate model can be found widely in the literature, for example in [16] or [17]. Assuming a fixed thickness h and the same fluid on both sides of the plate, the model depends only on 4 material parameters, namely the real part of the Young modulus E_r, the Poisson ratio ν, the density ρ and a

structural damping term η. The complex Young modulus is given by $E = E_r(1 + i\eta)$. For given pulsation ω and incidence angle θ, the impedance of the structure is

$$Z_s = -\omega^2 \rho h + D k_1^4, \tag{15}$$

where D is the bending stiffness of the plate defined as:

$$D = \frac{E h^3}{12(1-\nu^2)}, \tag{16}$$

and k_1 is the transverse part of the wavenumber. Due to the forced nature of the excitation, this quantity is constant through the system, and equal to the projection of the wave vector on the plate:

$$k_1 = k \sin\theta = \frac{\omega}{c_0} \sin\theta. \tag{17}$$

The acoustic transparency of the plate is defined as the ratio between transmitted and incident power per unit surface [**?**].

$$\tau(\omega, \theta) = \omega^2 Z_a^2 \frac{4}{|Z_s + 2i\omega Z_a|^2}, \tag{18}$$

where $Z_a = \rho_0 c_0 / \cos\theta$.

Introducing the coincidence pulsation:

$$\omega_{coin} = \frac{c_0^2}{\sin^2\theta} \sqrt{\frac{\rho_s h}{D}}, \tag{19}$$

equation 18 rewrites as:

$$\tau(\omega, \theta) = \frac{4 Z_a^2}{\omega^2 \rho_s^2 h^2 \left(1 - \frac{\omega^2}{\omega_{coin}^2}\right)^2 + \left(2 Z_a + \omega \rho_s h \eta \frac{\omega^2}{\omega_{coin}^2}\right)^2} \tag{20}$$

The sound transmission loss is defined as:

$$\mathrm{STL} = -10 \log_{10} \tau. \tag{21}$$

The frequency range can be divided into three different regions according to which parameter is dominant. They are separated by the coincidence frequency, defined by:

$$f_{coin} = \frac{1}{2\pi} \omega_{coin} \tag{22}$$

Classically, below f_{coin}, the transmission loss is governed by the mass law. Around coincidence, the drop in the TL is governed by damping, and in high frequencies the behavior is dominated by stiffness.

3.1.2 FAST Analysis

The FAST analysis was conducted on the above model for an infinite plate 1mm thick, with parameters uniformly distributed in the ranges defined in table 1. The computation of the main effects was done using 7,000 samples in the design range and an averaging over 3 repetitions, therefore 21,000 model evaluations, while that of the TSI necessitated 50,000 samples per parameter and repetitions, hence with 6 parameters and 5 repetitions, 300,000 model evaluations. The use of kriging metamodeling allowed it to reduce this number to just 1,000 evaluations per frequency range for both analyses.

Variable	Min. value	Max. value
E_x (GPa)	180	220
ν	0.27	0.33
ρ_s (kg.m^{-3})	7020	8580
η ($\cdot 10^{-3}$)	2.5	7.5

Table 1: Variation ranges of parameters for isotropic models

Results are presented in figure 2. As the considered model output is averaged over frequency bands, the sensitivity indices are plotted as histograms.

The dashed line represents the STL for the median values of the parameters (corresponding in this case to steel), divided by the maximum value over the whole range. This allows a visualization of the global trends of the model output for a special case. The three important zones are visible, below around and above coincidence.

The other interesting quantity shown on the graph is the normalized standard deviation (NSD), computed as the ratio of the global standard deviation to the mean value for each frequency band. A low NSD indicates that the function does not vary much in the given frequency and design ranges. It can be seen that outside coincidence range, NSD is usually practically 0, therefore optimization efforts should focus on this frequency range.

The density is shown to have a very high ME in low frequencies, while for higher frequencies, the Young modulus is predominant. This is consistent with the classical result that high frequencies are governed by stiffness effects and the low frequencies by mass effects.

As the design range has been chosen so that parameters lie within $\pm 10\%$ of typical values for steel, all coincidence frequencies occur rather close to each other.

A high level of interactions between parameters can be observed in the middle of the considered frequency range, where all parameters have rather low ME, but E and ρ exhibit high TSI. This high level of interaction can be explained by the fact that the coincidence frequency is characterized by an important drop in the TL, and that the value of this frequency (equation 19) is a function of both density and stiffness.

3.1.3 Influence of design range

The influence of the design space on the result has been studied by setting the damping range to $[2.5 \cdot 10^{-3}, 0.5]$. The results are given in figure 3. An increased influence of damping in the coincidence region is observed, as expected from the theory. There is practically no difference in the rest of the considered frequency range. However, varying more importantly the Young modulus and the density lead to a wider coincidence band, without changing the lower and higher frequency trends. This is due to the "local" effect of damping in the coincidence range, whereas the influence of mass and stiffness extend over much larger ranges.

In the context of the reduction of the number of parameters to be optimized, it may therefore be important to have a good prior knowledge of the uncertainties to which the parameters are subjected.

3.2 Diffuse field excitation

In the case of a diffuse field excitation, a superposition of plane wave with equiprobable incidence between 0 and $\pi/2$ is considered. The acoustic transparency is then:

$$\tau(\omega) = 2 \int_0^{\frac{\pi}{2}} \tau(\omega, \theta) \sin\theta \cos\theta \mathrm{d}\theta, \tag{23}$$

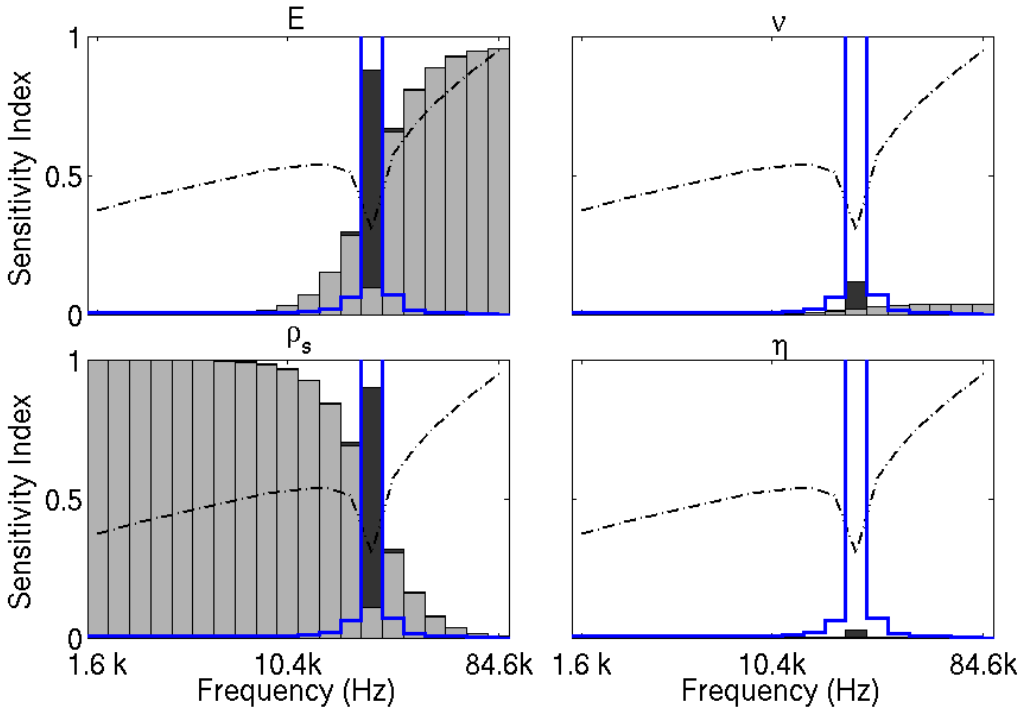

Figure 2: FAST sensitivity analysis of infinite isotropic plate under 45^o incident plane wave. Dark grey: TSI; Light grey: ME; dashed line: STL trend for the median plate; solid line: normalized standard deviation.

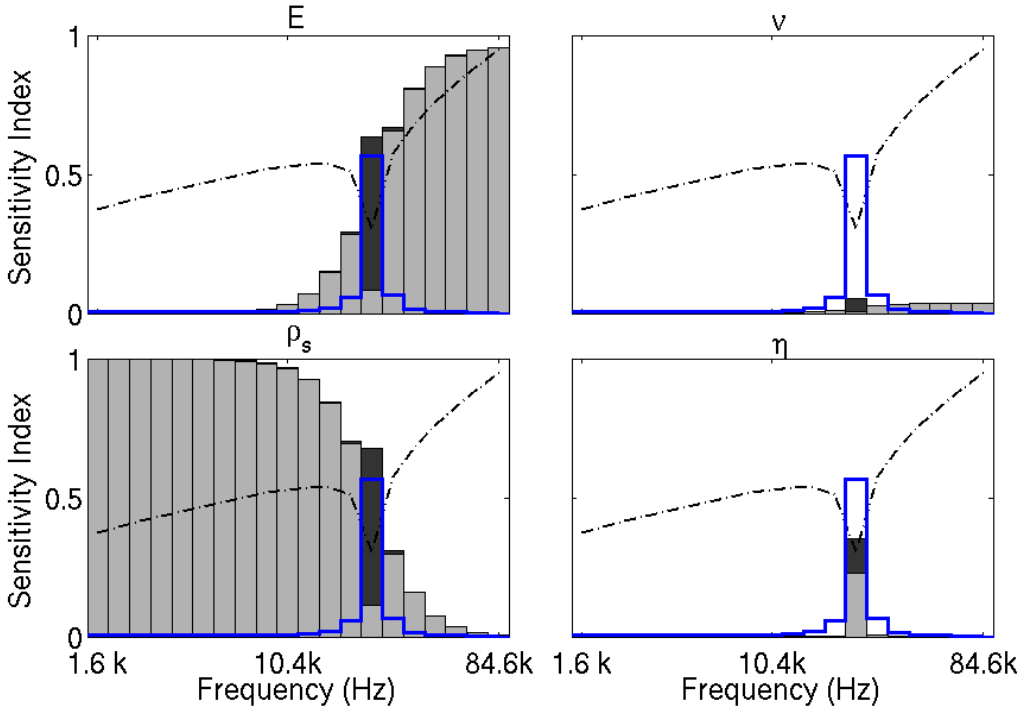

Figure 3: FAST sensitivity analysis of infinite isotropic plate under 45^o incident plane wave with high damping variability. Dark grey: TSI; Light gray: ME; dashed line: STL trend for the median plate; solid line: NSD

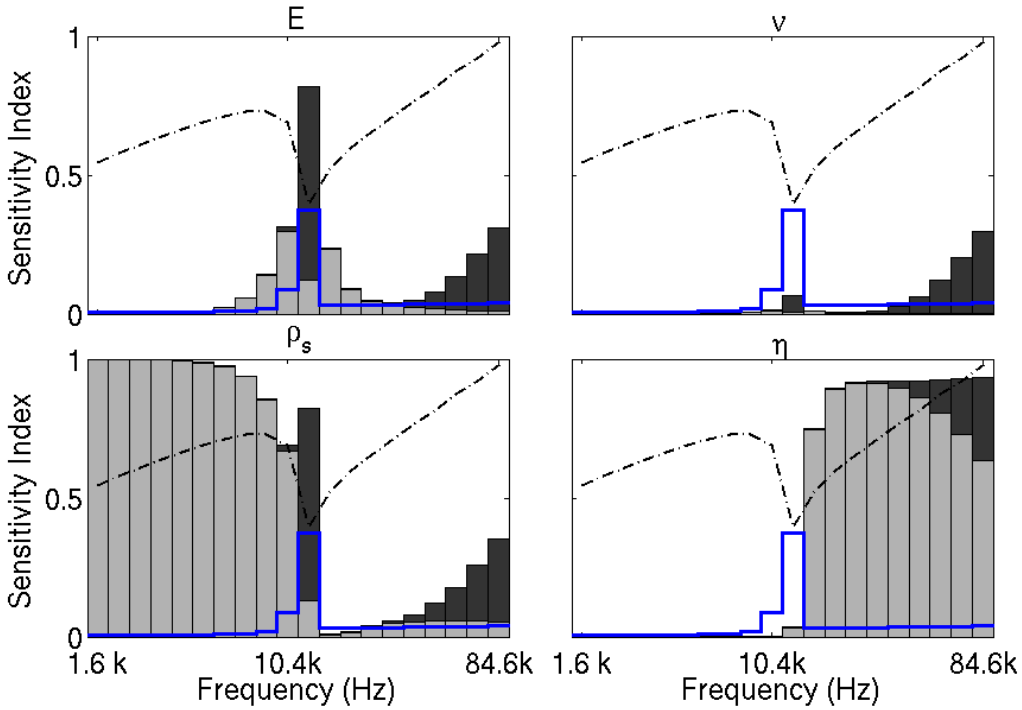

Figure 4: FAST sensitivity analysis of infinite isotropic plate under diffuse field excitation. Dark grey: TSI; Light gray: ME; dashed line: STL trend for the median plate; solid line: NSD

and the transmission loss is defined as in equation 21.

The diffuse field integration introduces a different behavior in the higher frequency range. Below f_{crit}, the mass law is still valid, but above it, the most influential parameter is by far damping, while stiffness parameters have an influence only on the location of the critical frequency

$$f_{crit} = f_{coin}(\theta = \pi/2). \tag{24}$$

This can be explained by the fact that above f_{crit}, coincidence occurs for some incidence at every frequency, so that the main effect governing the TL value is effectively the dip at coincidence, and no longer the coincidence frequency itself, so that damping becomes preponderant, even if it varies in the rather narrow range specified in table 1.

4 Orthotropic plate

4.1 Transmission loss under diffuse field excitation

The main difference with the isotropic case is in the expression of flexural stiffness, given in equation 16, which becomes for an orthotropic plate:

$$D_{ortho}(\varphi) = \left(C_{11}\sin^4\varphi + 2(C_{12}+2C_{33})\sin^2\varphi\cos^2\varphi + C_{22}\cos^4\varphi\right)\frac{h^3}{12} \tag{25}$$

Variable	Min. value	Max. value
E_x (GPa)	279	341
E_y (GPa)	5.89	7.15
G_{xy} (GPa)	3.87	4.73
ν	0.3285	0.4015
ρ_s (kg.m^{-3})	1.395	1.705
η ($\cdot 10^{-3}$)	2.5	7.5

Table 2: Variation ranges of parameters for orthotropic models

The terms of the stiffness matrix are defined as

$$\begin{aligned} C_{11} &= \frac{E_x}{1-\nu_{xy}\nu_{yx}} \\ C_{12} &= C_{11}\nu_{yx} \\ C_{22} &= \frac{E_y}{1-\nu_{xy}\nu_{yx}} \\ C_{33} &= G_{xy} \\ C_{23} &= C_{32} = C_{13} = C_{31} = 0 \end{aligned} \tag{26}$$

The transparency now has the same expression as equation 20, replacing D_{iso} by D_{ortho} in the expression of Z_s. As the transparency now also depends on heading direction φ, the diffuse field integration has to be done on both incidence angle and heading direction, hence:

$$\tau_d = \frac{1}{\pi}\int_{\varphi=0}^{2\pi}\int_{\theta=0}^{\frac{\pi}{2}} \tau(\omega,\varphi,\theta)\cos\theta\sin\theta\ \mathrm{d}\theta\mathrm{d}\varphi \tag{27}$$

4.2 FAST Analysis

The design range considered for the FAST analysis is based on the fibrous composite material M55J/M18 used in the aeronautic industry [18]. It is shown in table 2. An infinite plate of thickness 1cm is considered.

For an oblique incident plane wave the same trends as in the isotropic case can be observed. However, in diffuse field, two "critical frequencies" can be observed, corresponding to those in the main directions of the plate ($\varphi = 0$ and $\varphi = \frac{\pi}{2}$). Below this zone, the mass law approximation is valid, while above it, the same kind of damping control as in the isotropic case is observed. In the coincidence region, the transmission is a superposition of mass and damping-controlled modes, where the proportion of damping-controlled increases with frequency, hence the respective behavior of mass and damping sensitivities.

5 Conclusion

A global sensitivity method based on Analysis of Variance and Gaussian process metamodeling has been applied on acoustic transmission models of plates under oblique plane wave and diffuse field excitation.

The sensitivity is shown to be very different under these two excitation types in the higher frequency range. Indeed stiffness-like parameters are preponderant for plane wave excitation above coincidence, whereas damping is dominant for diffuse field in the same range. A more complex behavior is observed in the coincidence region of an orthotropic plate under diffuse field, where damping and mass have equivalent influence, due to the superposition of waves in their respective mass-controlled and damping-controlled ranges.

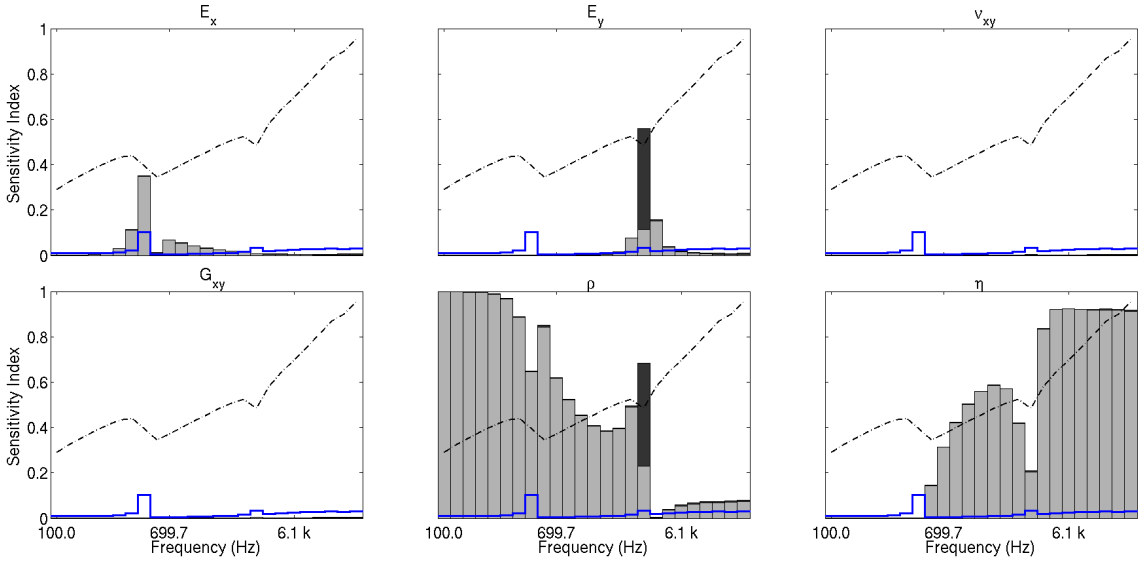

Figure 5: FAST sensitivity analysis of infinite orthotropic plate under diffuse field excitation. Dark grey: TSI; Light gray: ME; dashed line: STL trend for the median plate; solid line: NSD

This sensitivity analysis method thus allows to find the most influential parameters over a given frequency range. It is therefore an interesting preliminary step in the process of building a reduced model for optimization.

Acknowledgements

The authors would like to gratefully acknowledge Airbus Defence and Space for their financial support.

References

[1] J.-L. Guyader and C. Lesueur. *Transmission of reverberant sound through orthotropic viscoelastic multilayered plates*. *Journal of Sound and Vibration*, 70(3):319–332, 1980.

[2] L. R. Koval. *On sound transmission into an orthotropic shell*. *Journal of Sound and Vibration*, 63(1):51–59, 1979.

[3] D. Chronopoulos, M. Ichchou, B. Troclet, and O. Bareille. *Computing the broadband vibroacoustic response of arbitrarily thick layered panels by a wave finite element approach*. *Applied Acoustics*, 77:89–98, 2014.

[4] V. Cotoni, R.S. Langley, and P.J. Shorter. *A statistical energy analysis subsystem formulation using finite element and periodic structure theory*. *Journal of Sound and Vibration*, 318:1077–1108, 2008.

[5] T. Wang, S. Li, and S. R. Nutt. *Optimal design of acoustical sandwich panels with a genetic algorithm*. *Applied Acoustics*, 70:416–425, 2008.

[6] R. I. Cukier, C. M. Fortuin, K. E. Shuler, A. G. Petschek, and J. H. Schaibly. *Study of the sensitivity of coupled reaction systems to uncertainties on rate coefficients. I. Theory*. *Journal of Chemical Physics*, 59(8).

[7] B. Iooss, F. Van Dorpe, and N. Devictor. *Response surfaces and sensitivity analyses for an environmental model of dose calculations*. *Reliability Engineering and System Safety*, 91(10–11):1241–1251, 2006. The Fourth International Conference on Sensitivity Analysis of Model Output (SAMO 2004).

[8] M. Ouisse, M. Ichchou, S. Chedly, and M. Collet. *On the sensitivity analysis of porous material models*. *Journal of Sound and Vibration*, 331:5292–5308, 2012.

[9] A. Marrel, B. Iooss, F. Van Dorpe, and E. Volkova. *An efficient methodology for modeling complex computer codes with Gaussian processes*. *Computational Statistics and Data Analysis*, 52:4731–4744, 2008.

[10] A. Marrel, B. Iooss, B. Laurent, and O. Roustant. *Calculations of Sobol indices for the Gaussian process metamodel*. *Reliability Engineering and System Safety*, 94:742–751, 2009.

[11] H. Sathyanarayanamurthy and R. B. Chinnam. *Metamodels for variable importance decomposition with applications to probabilistic engineering design*. *Computers and Industrial Engineering*, 57:996–1007, 2009.

[12] S. N. Lophaven, H. B. Nielsen, and J. Sondergaard. DACE – A Matlab kriging toolbox, version 2.0. Technical report, Informatics and Mathematical Modelling, Technical University of Denmark, 2002.

[13] A. Saltelli, S. Tarantola, and K. P.-S. Chan. *A quantitative model-independent method for global sensitivity analysis of model output*. *Technometrics*, 41(1):39–56, 1999.

[14] B. Troclet, B. Hiverniau, M. Ichchou, L. Jezequel, K. Kayvantash, T. Bekkour, J. B. Mouillet, and A. Gallet. *FEM/SEA Hybrid Method for Predicting Mid and High Frequency Structure-Borne Transmission*. *The Open Acoustics Journal*, 2:45–60, 2009.

[15] Jack P.C. Kleijnen. *Kriging metamodeling in simulation: A review*. *European Journal of Operational Research*, 192(3):707–716, 2009.

[16] I. L. Ver and C. I. Holmer. *Noise and vibration control*, chapter 11: *Interaction of sound waves in solid structures*. edited by L. L. Beranek, McGraw-Hill, 1971.

[17] F. J. Fahy and P. Gardonio. *Sound and structural vibration*. Academic Press, 2007.

[18] G. Inquiété. *Simulation numérique de la propagation des ondes dans les structures composites stratifiées*. PhD thesis, École Centrale de Lyon, 2008.